

We are IntechOpen, the world's leading publisher of Open Access books Built by scientists, for scientists

6,900

Open access books available

185,000

International authors and editors

200M

Downloads

Our authors are among the

154

Countries delivered to

TOP 1%

most cited scientists

12.2%

Contributors from top 500 universities



WEB OF SCIENCE™

Selection of our books indexed in the Book Citation Index
in Web of Science™ Core Collection (BKCI)

Interested in publishing with us?
Contact book.department@intechopen.com

Numbers displayed above are based on latest data collected.
For more information visit www.intechopen.com



Design and Control of an EMG Driven IPMC Based Artificial Muscle Finger

R.K. Jain, S. Datta and S. Majumder

Additional information is available at the end of the chapter

<http://dx.doi.org/10.5772/48814>

1. Introduction

The medical, rehabilitation and bio-mimetic technology demands human actuated devices which can support in the daily life activities such as functional assistance or functional substitution of human organs. These devices can be used in the form of prosthetic, skeletal and artificial muscles devices (Andreasen et al., 2005; Bitzer & Smagt, 2006; DoNascimento et al., 2008). However, we still have some difficulties in the practical use of these devices. The major challenges to overcome are the acquisition of the user's intention from his or her bionic signals and to provide with an appropriate control signal for the device. Also, we need to consider the mechanical design issues such as lightweight and small size with flexible behavior etc (Arieta et al., 2006; Shenoy et al., 2008). For the bionic signals, the electromyography (EMG) signal can be used to control these devices, which reflect the muscles motion, and can be acquired from the body surface. We are familiar with the fact that ionic polymer metal composite (IPMC) has tremendous potential as an artificial muscle. This can be stimulated by supplying a small voltage of $\pm 3V$ and shows evidence of a large bending behavior (Shahinpoor & Kim, 2001; 2002; 2004; Bar-Cohen, 2002). In place of the supply voltage from external source for actuating an IPMC, EMG signal can be used where EMG electrodes show a reliable approach to extract voltage signal from body (Jain et al. 2010a; 2010b; 2011). Using this voltage signal via EMG sensor, IPMC can illustrate the bio-mimetic behavior through the movement of human muscles. Therefore, an IPMC is used as an artificial muscle finger for the bio-mimetic/micro robot.

The main objective of this chapter is to discuss the design and control of an IPMC based artificial muscle finger where this finger is actuated by EMG signal via movement of human finger. The movement is sensed by EMG sensor which provides signal for actuating the IPMC. When designing IPMC artificial muscle finger based micro gripper for handling the light weight components in an assembly, IPMC bending behaviour is utilized to hold the

object. During holding the object, stable EMG signal is required. For this purpose, stable EMG signal is sent through proportional–integral–derivative (PID) controller to the system. Experimentally, it is found that IPMC based artificial muscle finger achieves similar movement like human index finger. This IPMC based artificial muscle finger attains deflection upto 12 mm. By developing a prototype of IPMC artificial muscle finger based micro gripper, it is demonstrated that EMG driven system like IPMC artificial muscle finger based micro gripper can be applicable in handling of light weight components. The major advantages of such system are that IPMC based artificial muscle finger tip shows the compliant behavior and consumes less energy for actuation. Therefore, EMG driven system shows enough potential to substitute for conventional mechanism in micro manipulation and rehabilitation technology.

This chapter is organized as follows: Section 2 describes the prior research related to EMG applications in robotics and bio-mimetics. Section 3.1 explains the basic design of IPMC artificial muscle finger based micro gripper which is driven by EMG signal. The basic tendon of index finger is studied in section 3.2 where muscles are identified for actuation of IPMC based artificial muscle finger. In section 3.3, a model for controlling the EMG signal is highlighted. Different types of control system are implemented for achieving stable data from EMG signal via index finger which is sent to IPMC based artificial muscle finger. Section 4 discusses experimental testing setup for activation of IPMC based artificial muscle finger by human finger through EMG. In section 5, the results are discussed and the conclusions are drawn in section 6. The future work is recommended in section 7.

2. Prior research related to EMG applications

In the past, some researchers have reported work related to shape memory alloy (SMA) and other similar actuators to develop the bio-mimetic fingers but IPMC artificial muscle based finger related work is limited. Pfeiffer et al. (1999) have designed artificial limbs and robot prostheses that are lightweight, compact and dexterous. This mimics the human anatomy and maintains a high lifting capability. EMG control is used for SMA actuated fingers in robot prostheses. DeLaurentis & Mavroidis (2002) have discussed the design of a 12 degree-of-freedom (DOF) SMA actuated artificial hand where the SMA wires are embedded intrinsically within the hand structure. Cocaud & Jnifene (2003) have investigated the use of artificial muscles as SMA actuators for robot manipulators. A solution is established in order to determine the optimal position of a muscle in various musculoskeletal configurations. Herrera et al. (2004) have also designed and constructed a prosthesis where linear actuators are used for designing the mechanical system and EMG sensors are introduced for designing the electrical control system. Bundhoo et al. (2005, 2008) have reported the design of artificially actuated finger by SMA towards development of bio-mimetic prosthetic hands. Different finger joints are actuated through SMA wires via EMG and the relationship between elongation/contraction of the SMA wires & the finger joints have been obtained. O'Toole & McGrath (2007) have also focused on mechanical design of a 12 DOF SMA actuated artificial hand. The SMA material is used for combination of high strength

polymers such as polytetrafluoroethylene (PTFE), polyether ether ketone (PEEK) and low density metals such as titanium. Lau (2009) have carried out research work on a design and development of an intelligent prosthetic hand based on hybrid actuation through DC motor & SMA wires. These are controlled by myoelectric signal. Two novel features are introduced in the new prosthetic hand. Firstly, its hybrid actuation mechanism has the advantage of increasing the active degrees of freedom and secondly, using only two myoelectric sensors, has the potential for controlling more than three patterns of fingers movements. Pittaccio & Viscuso (2011) have developed a SMA wire device for the rehabilitation of the ankle joint where active orthosis powered by two rotary actuators like, NiTi wire are used to obtain ankle dorsiflexion and EMG signal is used to control the orthosis and trigger activation from muscle. Stirling et al. (2011) have shown the potential of SMA wire for an active, soft orthotic in the knee where NiTi based SMA wires is also used. A prototype is tested on a suspended, robotic leg to simulate the swing phase of a typical gait. Thayer & Priya (2011) have designed a biomimetic dexterous humanoid hand where the dexterity of the DART hand have been measured by quantifying functionality and typing speed on a standard keyboard. The hand consists of 16 servo motors dedicated to finger motion and three motors for wrist motion where some of joints are activated through SMA wires.

Some of the researchers have focused on the design of a biomechatronic robotic hand using EMG. Cheron et al. (1996) have found the relationship between EMG and the arm kinematics through dynamic recurrent neural networks (DRNN) method whereas Hudgins et al. (1997) have focused on a new control scheme, based on the recognition of naturally myoelectric signal patterns, transfers the burden of multifunction myoelectric control from the amputee to the control system. Rosen et al. (2001) have developed a myosignal-based exoskeleton system. This is implemented in an elbow joint, naturally controlled by the human. The human-machine interface is set at the neuromuscular level, by using the neuromuscular signal (EMG) as the primary command signal for the exoskeleton system. The EMG signals along with the joint kinematics are fed into a myoprocessor (Hill-based muscle model) which in turn predicts the muscle moments on the elbow joint. Banks (2001) has given remarkable effort towards design and control of an anthropomorphic robotic finger with multi-point tactile sensation whereas Light et al. (2002) have emphasized on intelligent multifunction myoelectric control of hand prostheses. Peleg et al. (2002) have extracted multiple features via EMG signal from hand amputees which is selected by help of a genetic algorithm. Fukuda et al. (2003) have developed a prosthetic hand where human-assisting manipulator system based on the EMG signals is utilized. Wheeler (2003) has presented a neuro-electric interface method for virtual device control. The sampled EMG data is taken from forearm and then is fed into pattern recognition software that has been trained to distinguish gestures from a given gesture set. Kryzstoforski et al. (2004) have given remarkable effort towards recognition of palm finger movements on the basis of EMG signals with the application of wavelets.

Crawford et al. (2005) have used EMG signals for classifying in real-time with an extremely high degree of accuracy in a robotic arm-and-gripper. A linear support vector machines (SVM) based classifier and a sparse feature representation of the EMG signal are used.

Hidalgo et al. (2005) have proposed a design of robotic arm employing fuzzy algorithms to interpret EMG signals from the flexor carpi radialis, extensor carpi radialis and biceps brachii muscles. The control and acquisition systems are composed of a microprocessor, analog filtering, digital filtering & frequency analysis, and finally a fuzzy control system. Mobasser & Hashtrudi-Zaad (2005) have estimated rowing stroke force with EMG signal using artificial neural network method from upper arm muscles which is involved in elbow joint movement, sensed elbow angular position and velocity. Gao et al. (2006) have focused on acquiring the data from the upper limb of the body for robotic arm motion using EMG whereas Frigo et al. (2007) have detected EMG signal from voluntarily activated muscles which is controlled for functional neuromuscular by electrical stimulation. A comb filter (with and without a blanking window) is applied to remove the signal components synchronously correlated to the stimulus. Roy et al. (2007) have compared the performance of different sEMG signal at various conditions. These performances depend on the electro-mechanical stability between the sensor and its contact with skin. Zollo et al. (2007) have put a remarkable effort on the control system of biomechatronic robotic hand and on the optimization of the hand design in order to obtain human like kinematics and dynamics. By evaluating the simulated hand performance, the mechanical design is iteratively refined. The mechanical structure and the ratio between numbers of actuators to the number of DOF have been optimized. Yagiz et al. (2007) have developed a dynamic model of the prosthetic finger where a non chattering robust sliding mode control is applied to make the model follow a certain trajectory. Wege & Zimmermann (2007) have shown the potential of EMG control for a hand exoskeleton device. The device has been developed with focus on support of the rehabilitation process after hand injuries or strokes. Itoh et al. (2007) have studied the hand finger operation using sEMG during crookedness state of the finger. Two electrodes (Ag/AgCl electrodes) are stucked randomly on the forearm muscles and the intensity of EMG signals at different muscles is measured for each crooked finger.

Hao et al. (2008) have studied the design of pneumatic muscle actuator based robotic hand where its compliance and dexterity handling are attempted. A single finger is controlled by fuzzy & PID controller and comparative studies are discussed. Murphy et al. (2008) have explored the micro electro-mechanical systems based sensor for mechanomyography system whereas Saponas et al. (2008) have also explored the feasibility on muscle-computer interaction methodology that directly senses and decodes human muscular activity rather than relying on physical device actuation or user actions. Andrews (2008) has determined an effective approach to finger movement classification in typing tasks using myoelectric data which are collected from the forearm. Cesqui et al. (2008) have explored the use of EMG signals for post-stroke and robot-mediated therapy. In this work, a pilot study has been reported under young and healthy subjects where experiments are conducted to determine whether it is possible to build a static map to cluster EMG activation patterns for horizontal reaching movements. Chen et al. (2008) have implemented an EMG feedback control method with functional electrical stimulation cycling system (FESCS) for stroke patients. The stroke patients often suffer from low limbs paralysis. By designing the feedback control protocol of FESCS, the physiological signal is recorded with help of FPGA biomedical module, DAC and electrical stimulation circuit. Lee et al. (2009) have described a

development procedure of bio-mimetic robot hand and its control scheme where each robot hand has four under-actuated fingers, which are driven by two linear actuators coupled together. Dalley et al. (2009) have given emphasis of an anthropomorphic hand prosthesis that is intended for use with a multiple-channel myoelectric interface. The hand contains 16 joints, which are differentially driven by a set of five independent actuators. Hu et al. (2009) have presented a comparison between electromyography-driven robot and passive motion device on wrist rehabilitation for chronic stroke patients. By comparative study, it was found that the EMG-driven interactive training had a better long-term effect than the continuous passive movement (CPM) treatment.

Blouin et al. (2010) have focused on control of arm movement during body motion as revealed by EMG whereas Luo & Chang (2010) have explored a feasibility study on EMG signal integrated with multi-finger robot hand control for massage therapy applications. The forearm EMG of a person massaged by the human hands is recorded and analyzed statistically. Khokhar et al. (2010) have showed the potential of EMG applications where SVM classification technique is suitable for real-time classification of sEMG signals. This technique is effectively implemented for controlling an exoskeleton device. Huang et al. (2010) have designed a robust EMG sensing interface for pattern classification. The aim of this study was to design sensor fault detection (SFD) module through the sensor interface to provide reliable EMG pattern classification. This module monitors the recorded signals from individual EMG electrodes and performs a self-recovery strategy to recover the classification performance when one or more sensors are disturbed. Naik et al. (2010) has studied the pattern classification of myo-electric signal during different maximum voluntary contractions using BSS techniques for a blind person whereas Artemiadis & Kyriakopoulos (2010 & 2011) have presented a switching regime model for the EMG-based control of a robot arm where decode the EMG activity of 11 muscles has a continuous representation of arm motion in the 3-D space. The switching regime model is used to overcome the main difficulties of the EMG-based control systems, i.e. the nonlinearity of the relationship between the EMG recordings and the arm motion, as well as the non-stationary of EMG signals with respect to time. Vogel et al. (2011) have demonstrated the robotic arm/hand system that is controlled in real time in 6 dimension Cartesian space through measured human muscular activity via EMG. DLR Light-weight Robot III is used during demonstration of impedance control. Li et al. (2011) have presented a robot control system using four different gestures from an arm. These are achieved by EMG signal using phase synchrony features. The phase synchrony analysis using the recent multivariate extensions of empirical mode decomposition (MEMD) is carried out. Joshi et al. (2011) have focused on brain-muscle-computer interface using a single sEMG signal. Initial results show that the human neuromuscular system can simultaneously manipulate partial power in two separate frequency bands of a sEMG power spectrum at a single muscle site. Matsubara et al. (2011) have proposed an interface to intuitively control robotic devices using myoelectric signals. Through learning procedure, a set of myoelectric signals is captured from multiple subjects in the system and it can be used as an adaptation procedure to a new user after only a few interactions.

Recently, Ahmad et al. (2012) have presented a review report on different techniques of EMG data recording where condition of an ideal pre-amplifier, signal conditioning and its amplification are discussed. Sun et al. (2012) have conducted an isokinetic exercise to realize the characteristics of femoral muscles in human knee movement through EMG where a mechanical model of muscle for human knee movement is established. Qi et al. (2012) have developed algorithms for muscle-fatigue detection and muscle-recruitment patterns in routine wheel chair propulsion scenarios, e.g., daily practice where for analysis purpose two speeds of muscular behavior are chosen. Gandole (2012) has developed an artificial intelligent model using focused time lagged recurrent neural network (FTLRNN) method with a single hidden layer. FTLRNN method reduces noise intelligently from the EMG signal. Chan et al. (2012) have developed an assessment platform for upper limb myoelectric prosthetic devices using EMG. The assessment platform consists of an acquisition module, a signal capture module, a programmable signal generation module and an activation & measurement module. The platform is designed to create a sequence of activation signals from EMG data captured from a patient.

An EAP actuator based design for IPMC fingers have been discussed by Biddiss & Chau (2006). This shows the potential of electroactive polymeric sensors within an operating range of voltage ($\pm 3V$) whereas Kottke et al. (2007) have reported on how to stimulate and activate a non-biological muscle such as an IPMC. Lee et al. (2006, 2007) have also demonstrated the potential of an IPMC actuating system with a bio-mimetic function using EMG signals. A mean absolute method is used for achieving the filtered EMG signal. Aravinthan et al. (2010) have designed a multiple axis prosthetic hand using IPMC. EMG signal through programmable interface controller (PIC) is sent to the IPMC prosthetic material to perform the required actions. By doing experiments, the potential of prosthetic hand using IPMC is shown. After that, we have also demonstrated actuation of IPMC through EMG via forearm muscles where potential of IPMC based micro robotic arm has been shown for lifting the object (Jain et al., 2010a; 2010b; 2011; 2012). For further application of EMG driven system, we are discussing detailed analysis of EMG signal control point view of IPMC based artificial muscle finger for micro gripper in this chapter.

3. Design and control of IPMC based artificial finger driven by EMG signal

3.1. Basic design of IPMC artificial muscle finger based micro gripper using EMG

For designing an IPMC artificial muscle finger based micro gripper using EMG, an IPMC strip (Size 40 mm \times 10 mm \times 0.2 mm) that imitates human finger movement, is assumed to be artificial muscle finger. This is fixed with holder and another plastic based finger of similar size is made for supporting the micro object as shown in Fig. 1. When human index finger moves up and down, it creates potential difference by its movements. This potential difference is transferred through EMG electrodes into the artificial muscle finger so that this finger is able to move accordingly and hold the object. The main function of EMG electrode

is to detect the voltage from human muscles since human muscles generate few millivolts when they are contracting or expanding during movement. For transferring this voltage signal to actuate the artificial muscle finger, it needs the amplification setup which is discussed in section 4. Therefore, IPMC based artificial muscle finger is activated using EMG and it allows holding an object for micro assembly operation.

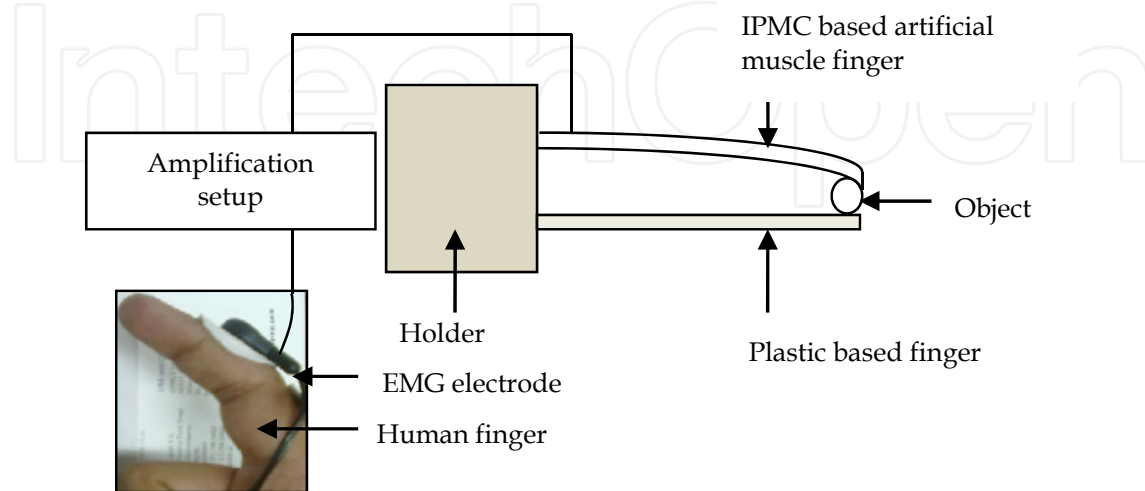


Figure 1. Schematic diagram of IPMC artificial muscle finger based micro gripper driven by EMG

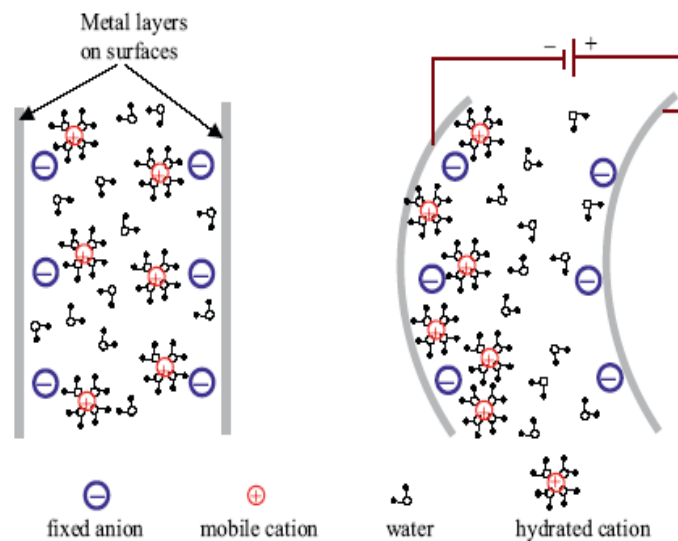


Figure 2. Schematic diagram of the actuation mechanism of IPMC (Chen et al., 2011)

During development of an EMG driven IPMC based artificial muscle finger, a typical IPMC strip (Procured custom made from Environmental Robots Inc., USA) is used which has a thin (approximately 200 μm) perfluorinated ion exchange base polymer membrane (Nafion-117) with metal electrodes of platinum (5–10 μm) fused on either side. As a part of the manufacturing process, this base polymer is further chemically coated with metal ions that comprise the metallic composites. It responds in wet/dry condition. An IPMC is usually kept in a hydrated state to ensure proper dynamic operation. When the material is hydrated, the cations will diffuse toward an electrode on the material surface under an applied electric

field. Inside the polymer structure, anions are interconnected as clusters providing channels for the cations to flow towards the electrode (Chen et al., 2011). This motion of ions causes the structure to bend toward the anode as shown in Fig. 2. An applied electric field affects the cation distribution within the membrane, forcing the cations to migrate towards the cathode. This change in the cation distribution produces two thin layers, one near the anode and another near the cathode boundaries. The potential is generated by changing the potential electric field on cluster of ionic strips that provides the actuation of the strip.

3.2. Basic tendon of index finger for identification of EMG signal

To examine the bio-mimetic behavior of IPMC based artificial muscle finger, it is important to study the physiological structure of human finger. An internal structure of human index finger is shown in Fig. 3. The index finger is actuated by three intrinsic muscles and four extrinsic muscles. The intrinsic muscles consist of two interosseous (IO 1 and IO 2) muscles & one lumbrical (LU) muscle and four extrinsic muscles connected through long tendons i.e. extensor digitorum communis (EDC), extensor indicis proprius (EIP), flexor digitorum superficialis (FDS) and flexor digitorum profundus (FDP) (Bundhoo & Park, 2005). For heavy lifting & holding purpose, EDC and EIP are responsible in tendon network. Consequently, EMG electrodes are placed at these two positions on the human finger so that we can achieve direct actuation of IPMC based artificial muscle finger through said muscles.

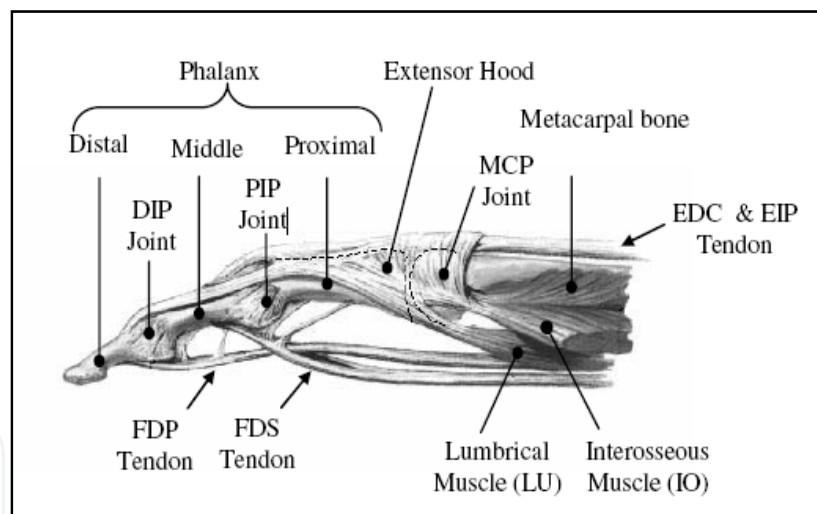


Figure 3. Basic tendons of the index finger (Bundhoo & Park, 2005)

3.3. Model for controlling the EMG signal for IPMC based artificial muscle finger

For acquiring the data from said muscles, EMG electrodes are placed for measuring the electric potential produced by voluntary contraction of muscle fiber on the human finger. The frequency range of the EMG signal is within 4 to 900 Hz. The dominant energy is concentrated in the range of 95 Hz and amplitude of voltage range is ± 1.2 mV according to muscle contraction and the voltage function $V_{in}(t)$ in term of signal sample time (t) is given below,

$$V_{in}(t) = V_{ino} \sin(2\pi ft) \tag{1}$$

Where, V_{ino} is amplitude of EMG voltage (± 0.0012 V); f is frequency of EMG signal (95 Hz).

In Laplace domain, EMG input signal is written as

$$V_{in}(s) = \frac{2.96}{s^2 + 3.51e5} \tag{2}$$

Using these parameters, the circuit for filtered EMG signal is designed using MATLAB SIMULINK software as shown in Fig. 4.

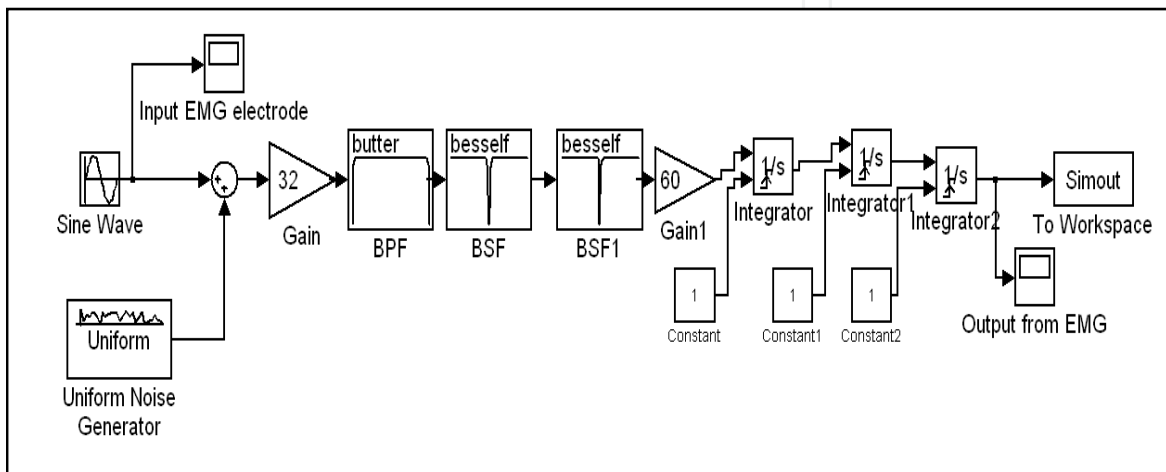


Figure 4. Block diagram of EMG signal behaviour from human index finger

In block diagram, the active EMG signal is taken from index finger muscle and uniform noise is considered. The electric potential is first amplified with gain 32 dB and then band pass filter (BPF) is used within specified frequency range (4 to 900 Hz). Using two band stop filters (BSF and BSF1), noise signal (60 Hz) that arises due to AC coupled power is eliminated. The signal is then passed through an amplifier with gain 60 dB. Subsequently, three integrators (Integrator, Integrator1 and Integrator2) are used for achieving better damped signal. The output of EMG signal with sampling time of 10^{-4} seconds after filtering is shown in Fig. 5.

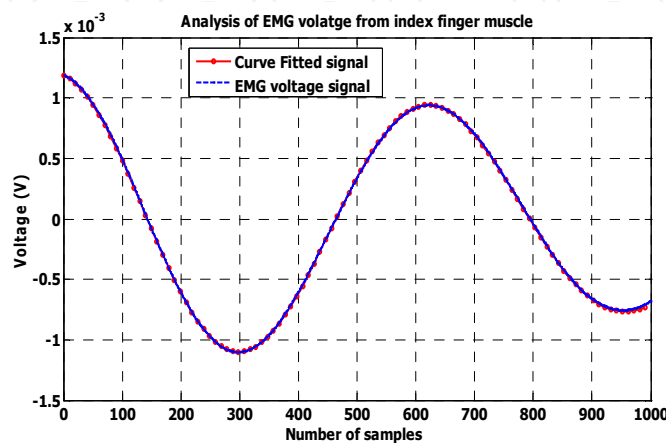


Figure 5. Acquired data from finger muscles via EMG signal

Thus, the total output duration of EMG signal for sampled data is 0.1 second. The general solution of acquired EMG voltage (V_{EMG}) through curve fitting method is obtained as given below,

$$V_{EMG}(t) = \sum V_0 \sin(2\pi f_0 t + \delta_0), \quad 0 \leq t \leq 0.1 \quad (3)$$

where, V_0 is the amplitude of EMG voltage of sine function (± 0.0012 V); f_0 is average frequency of sine function (4.7 Hz); δ is initial phase difference of sine function (1.66 rad); t is signal sample time in second.

After adjustment of root mean square (RMS) value of this sine function, the EMG voltage $V_{EMGrms}(s)$ after filtering is written as

$$V_{EMGrms}(s) = \frac{1.16e^{-5}(s^2 + 1.17e^{-4})}{(s^2 - 0.014s + 1.07e^{-4})(s^2 + 0.014s + 1.07e^{-4})} \quad (4)$$

For controlling purpose, single input single output (SISO) control system tool in MATLAB is used and the output $V_{EMG}(s)$ data is obtained. The initial overall transfer function of EMG voltage $V_{EMGinitial}(s)$ is obtained through output signal from (4) to input signal from (2) and is given as

$$V_{EMGinitial}(s) = \frac{3.92e^{-6}(s^2 + 1.17e^{-4})(s^2 + 3.5e^5)}{(s^2 - 0.0146s + 1.07e^{-4})(s^2 + 0.0146s + 1.07e^{-4})} \quad (5)$$

After that, Nyquist criterion is applied to check the stability of EMG signal. The root-locus and bode scheme are plotted as shown in Fig. 6.

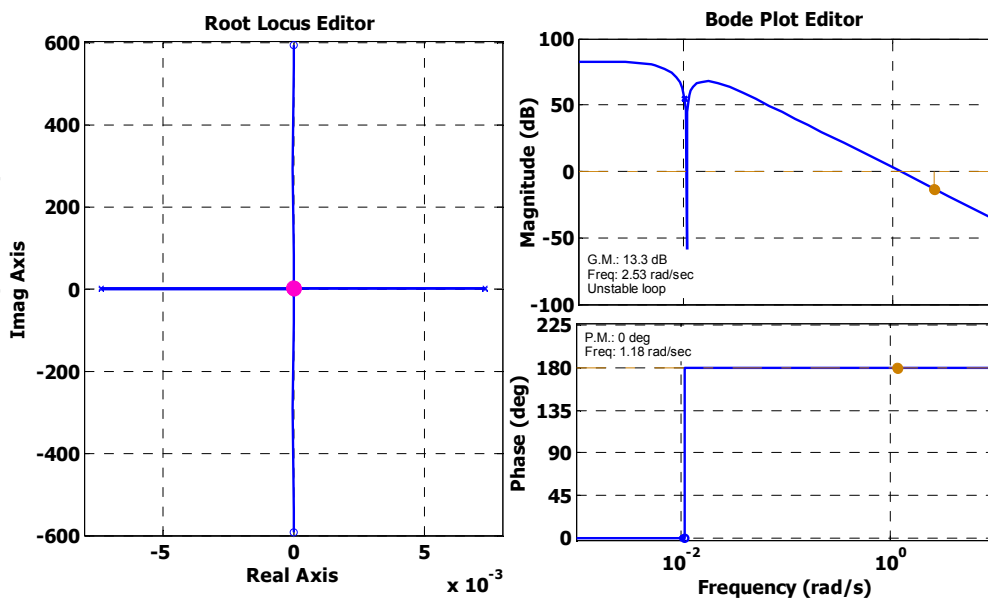


Figure 6. Root-locus and bode plot behaviour of EMG signal via finger in initial condition (Jain et al., 2011)

It is found that the zero-poles have real value on both sides of the real axis which does not meet the Nyquist stability criteria. Also from Fig. 6, gain cross-over frequency (GCF=2.53 rad/s) is greater than phase cross-over frequency (PCF=1.18 rad/s), indicating that this voltage obtained from EMG signal is unstable.

For achieving the stable EMG signal, different configurations of PID are analysed through SISO control tool of MATLAB software. By applying PD control with proportional control gain factor ($K_p=1$) and derivative control gain factor ($K_d=1$), EMG voltage $V_{EMGfinal1}(s)$ is obtained as given below,

$$V_{EMGfinal1}(s) = \frac{(s^2 + 1.17e^{-4})(s^2 + 3.516e^5)}{(s + 2.546e^5)(s^2 - 9.91e^{-9}s + 1.17e^{-4})(s^2 + 1.38s + 1.38)} \quad (6)$$

The root locus and bode plot are shown in Fig. 7. This indicates that the obtained data from EMG signal is unstable but through this control system the data is converging towards stability from initial condition.

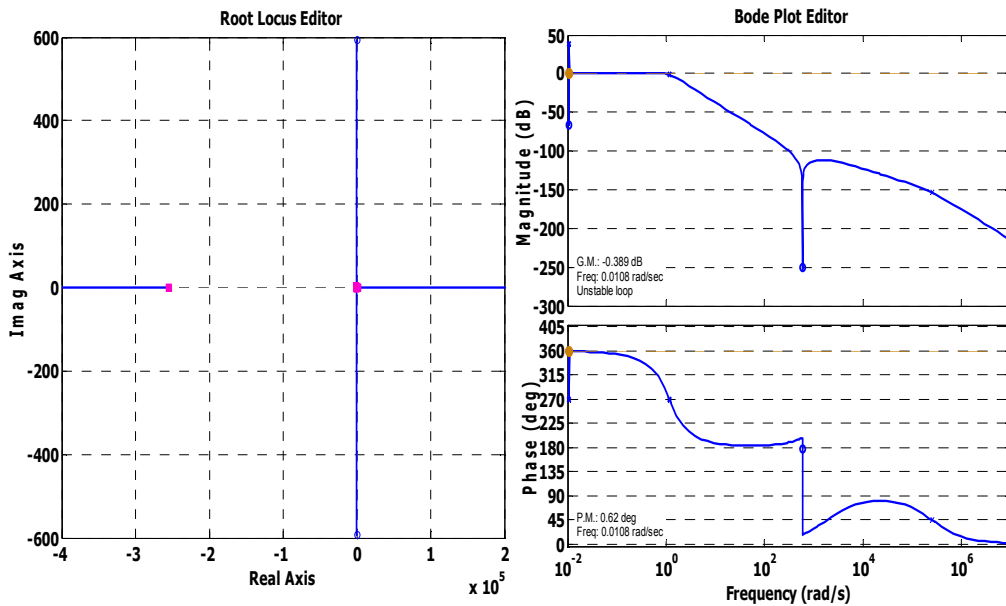


Figure 7. Root-locus and bode plot behaviour of human finger through PD controller

In case of PI controller, the unit proportional control gain factor ($K_p=1$) and integrator control gain factor ($K_i=1$) parameters are used. After applying this control system, EMG voltage $V_{EMGfinal2}(s)$ is obtained as given below,

$$V_{EMGfinal2}(s) = \frac{3.92e^{-6} s (s^2 + 1.17e^{-4})(s^2 + 3.51e^5)}{(s + 0.724)(s^2 + 9.91e^{-9}s + 1.17e^{-4})(s^2 - 0.724s + 1.90)} \quad (7)$$

The bode plot and root locus for this system are plotted as shown in Fig. 8. From this figure, it shows that the data from EMG signal is again unstable but the response has a better prospect of converging towards stability than previous configuration.

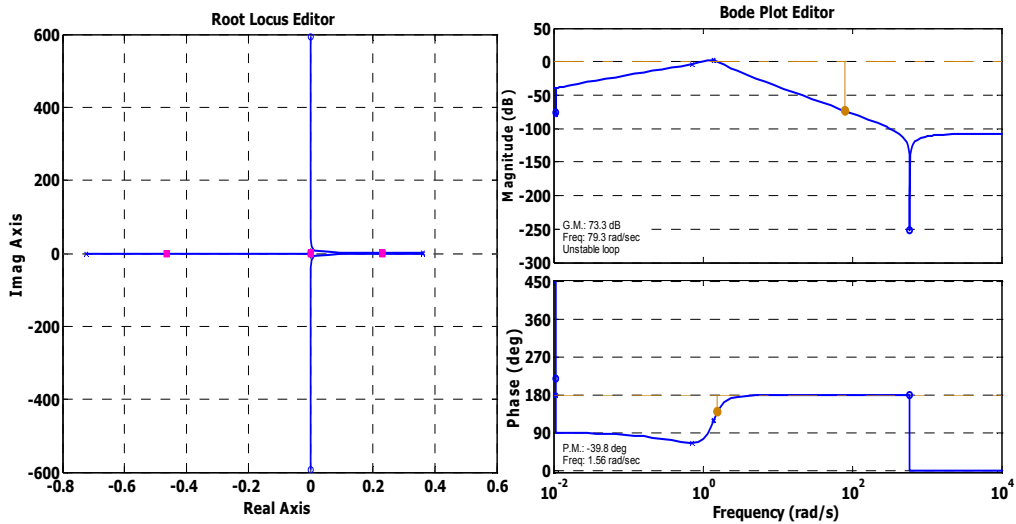


Figure 8. Root-locus and bode plot behaviour of EMG signal via finger through PI controller

After that, PID controller is used where proportional control gain factor ($K_p=0.5$), integrator control gain factor ($K_i=1$) and derivative control gain factor ($K_d=1$) are given in compensator to attain the stability of EMG voltage. For applying the PID control system, the SIMULINK block diagram is modified as shown in Fig. 9.

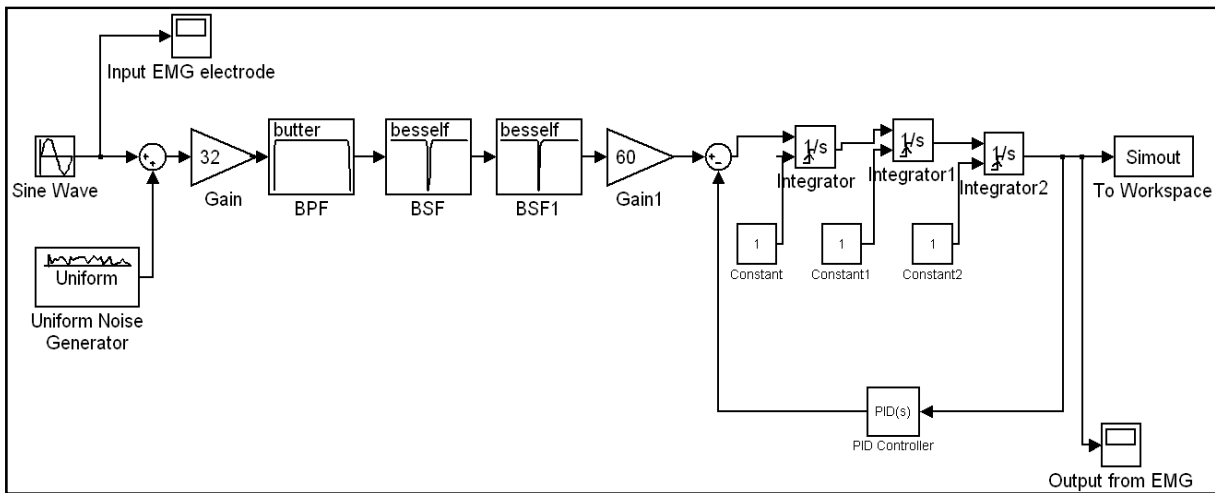


Figure 9. Block diagram of EMG signal via human finger after applying PID control system

Thereafter, the model is again simulated in MATLAB software, upon which, the data from finger muscles shows the all zero-poles in left hand side of real axis which satisfies the Nyquist criteria shown in Fig. 10. The final EMG voltage $V_{EMGfinal}(s)$ is acquired as given below,

$$V_{EMGfinal}(s) = \frac{s (s^2 + 1.17e^{-4})(s^2 + 3.51e^5)}{(s + 2.54e^5)(s + 1.52)(s^2 + 1.83e^{-8}s + 1.17e^{-4})(s^2 - 0.14s + 0.90)} \quad (8)$$

Also, GCF (1rad/s) is less than PCF (1.34 rad/s). Hence, a stable EMG voltage data is achieved. This filtered EMG signal is stable enough to provide necessary voltage signal across the IPMC for proper functioning during operation. The major advantage of this

control system is that it is stable with least amount of noise. This signal is sent to artificial muscle finger for holding the object.

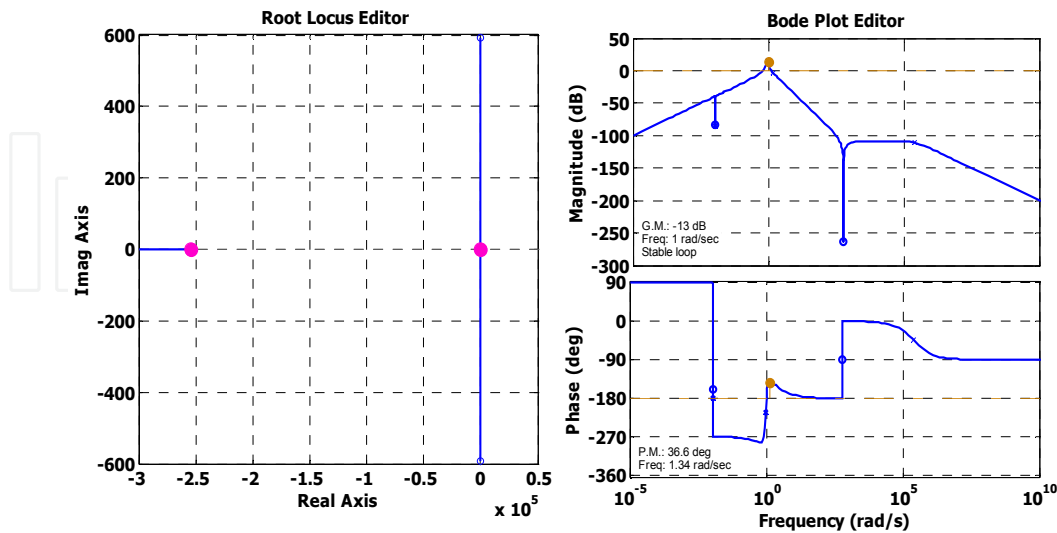


Figure 10. Root-locus and bode plot behaviour of EMG signal via finger through PID controller (Jain et al., 2011)

4. Experimental testing setup

In order to examine the bio-mimetic behaviour of IPMC based artificial muscle finger through EMG signal, EMG electrodes (Ag/AgCl based) are positioned at EDC and EIP muscles on the index finger. The input EMG signal from the muscle movement varies in the range of $\pm 1.2\text{mV}$ (which is observed through oscilloscope). But activation of IPMC based artificial muscle finger needs the voltage of $\pm 3\text{V}$ and current rating of 50-200 mA which is only possible by amplification of voltage and current. For desired output voltage to the artificial muscle finger, EMG signal is transferred through analog-digital convertor (ADC) card and PXI system (PXI-1031 along with NI-6289) in real time environment. EMG signal through electrodes are sent to an input channel at specified ports of the ADC card. Then this signal is amplified through amplification factor of 2550 using express VI of Labview 8.5 and sent to DAC output. But DAC output signal cannot provide enough current (50-200 mA) to drive an IPMC based artificial muscle finger. For achieving this current rating, the current amplification is done using customized IPMC control circuit by combining operational amplifier (Model: LM-324), transistor (Model: TIP 122) and resistances ($1\text{k}\Omega$ and 10Ω). Noise interference is eliminated by enabling low-pass filtering with PID control system to achieve the stability during operation of the artificial muscle finger as shown in Fig. 11. The IPMC size $40\text{mm} \times 10\text{mm} \times 0.2\text{mm}$ is used for testing purpose.

Now, in order to prevent the abrupt physio-chemical change of the IPMC nature and subsequent shortening of the actuation operating time of the IPMC material due to irreversible electrolysis (caused when the voltage applied across the two faces of an IPMC exceeds a maximum limit), two warning flags are used. One warning flag is placed at input EMG signal and another warning flag is placed at output voltage of DAC card where IPMC control circuit is connected. This limited voltage imposed on the IPMC based artificial muscle finger aborts

the execution of the program when the warning flag has a high output. The flow chart for actuation of IPMC based artificial muscle finger is shown in Fig. 12. During operation, artificial muscle finger bends in a similar manner as that of the index finger. For generating force, this finger is held in cantilever configuration on the fabricated work bench. A load cell is used to collect the data at different angles of the index finger. The current and voltage analysis of the human muscles are also done through oscilloscope. Thus an IPMC artificial muscle finger based micro gripper driven by EMG is developed and the holding behaviour is demonstrated.

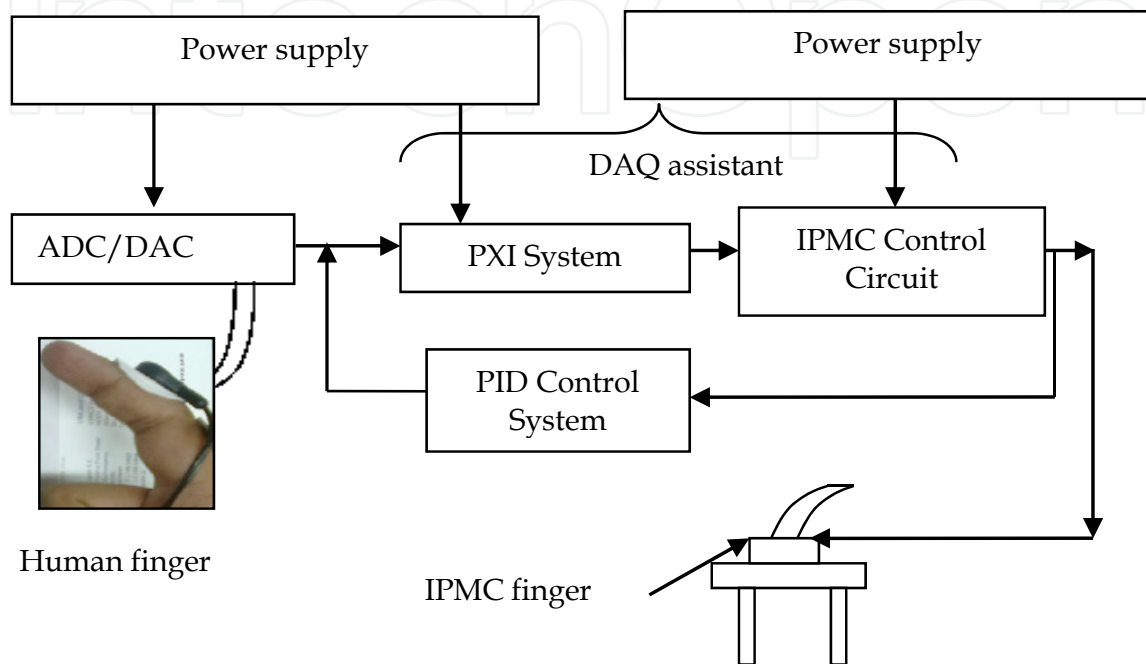


Figure 11. Basic testing layout for actuation of IPMC based artificial muscle finger

5. Results and discussion

During experimentation, the input parameter from muscle ranging from ± 1.2 mV is taken through referenced single-ended (RSE) signal along with continuous sampled pulses. These pulses are amplified with the help of a PXI system (amplification factor 2550). The desired output voltage range is generated through a DAC output port. The output signal is connected to IPMC based artificial muscle finger. Due to amplified output voltage from the DAC, an IPMC strip bends in one direction for holding the object. By changing the movement of human finger in an opposite direction, reverse behaviour of IPMC is obtained. The characteristics of IPMC based artificial muscle finger are traced on a graph paper and plotted as shown in Fig. 13. It shows that IPMC based artificial muscle finger gives similar bending behaviour as a human finger (Fig. 14). It is also observed that the deflection of IPMC based artificial muscle finger changes with voltage upto 12 mm in one direction. When this finger moves reverse direction, the characteristic of artificial finger does not attempt the same behaviour. It shows the error between two paths is 0.5 mm. The deflection characteristic of IPMC based artificial muscle finger (δ) in term of voltage (V) with cubic behaviour for holding is given below,

$$\delta(V) = 0.67 \times V^3 - 1.9 \times V^2 + 3.7 \times V - 0.17 \quad (\text{in mm}) \quad (9)$$

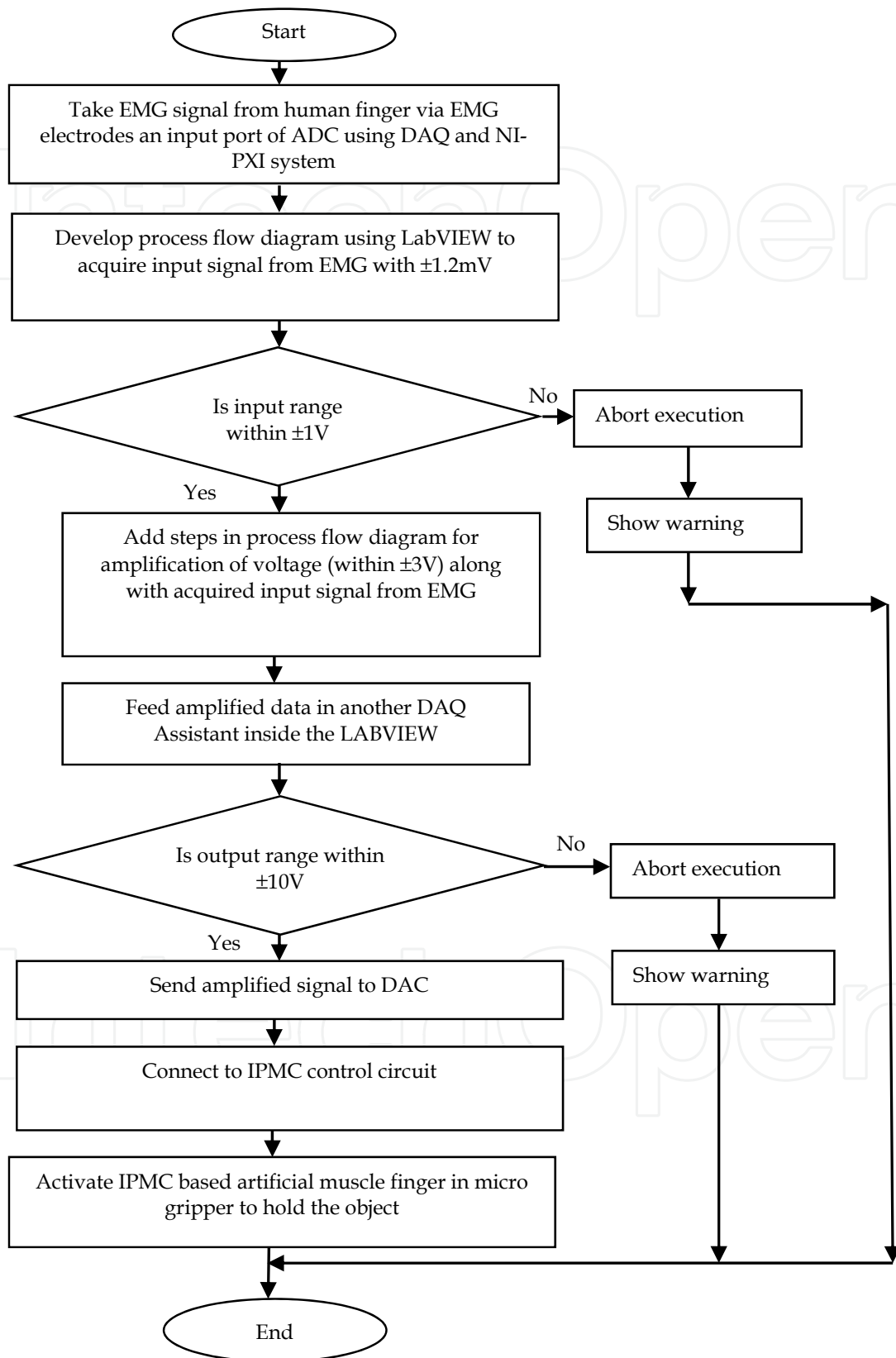


Figure 12. Flow chart of for actuation IPMC based artificial muscle finger using EMG signal

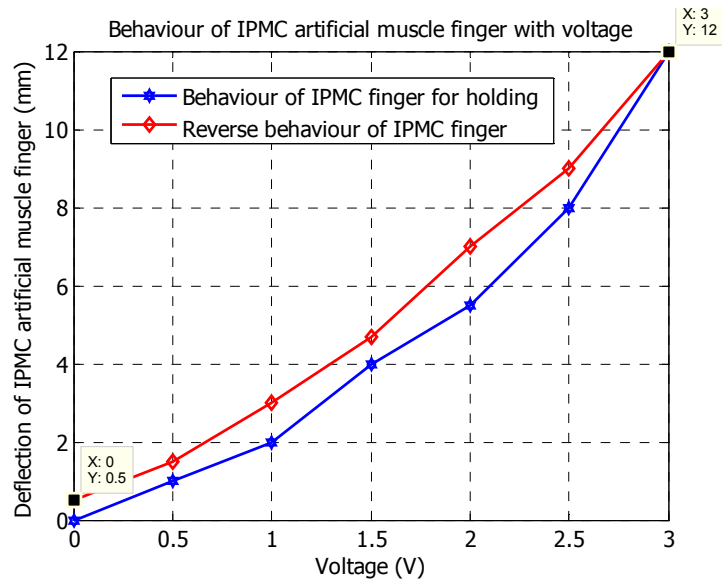


Figure 13. Deflection behaviour of IPMC based artificial muscle finger with different voltages

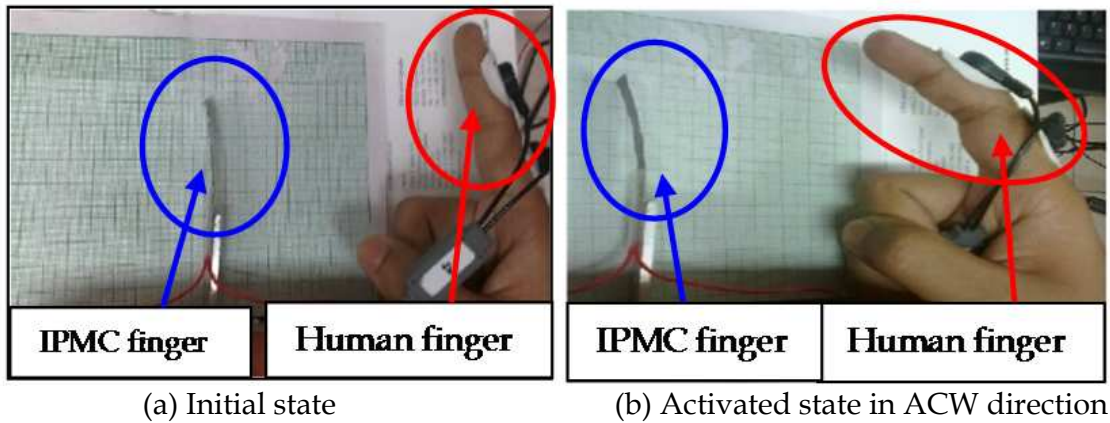


Figure 14. Control of IPMC based artificial muscle finger through EMG signal (Jain et al., 2011)

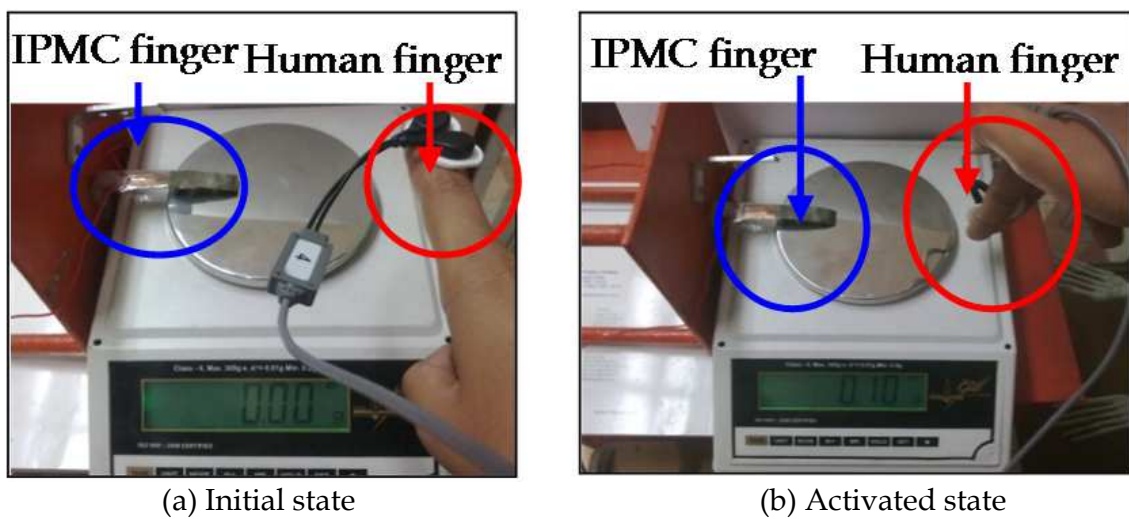


Figure 15. Load test setup for IPMC based artificial muscle finger using load cell

For generating force by the artificial muscle finger, a testing setup with load cell is used. The IPMC based artificial muscle finger is placed in cantilever mode, and a load cell is placed under the tip of the IPMC which produces the reactive force. When human finger moves downward, the generated force by IPMC artificial muscle finger increases accordingly in the load cell as shown in Fig. 15.

By controlling the movement of human finger, the generated force varies accordingly. The generated force characteristic with voltage shows a cubic polynomial behaviour as shown in Fig. 16 when IPMC artificial muscle finger touches the load cell. This happens due to compliant behaviour of IPMC. The generated force (F) by IPMC based artificial muscle finger in term of voltage (V) is given below,

$$F(V) = 0.11 \times V^3 + 0.25 \times V^2 + 1.6 \times V - 0.11 \quad (\text{in mN}) \quad (10)$$

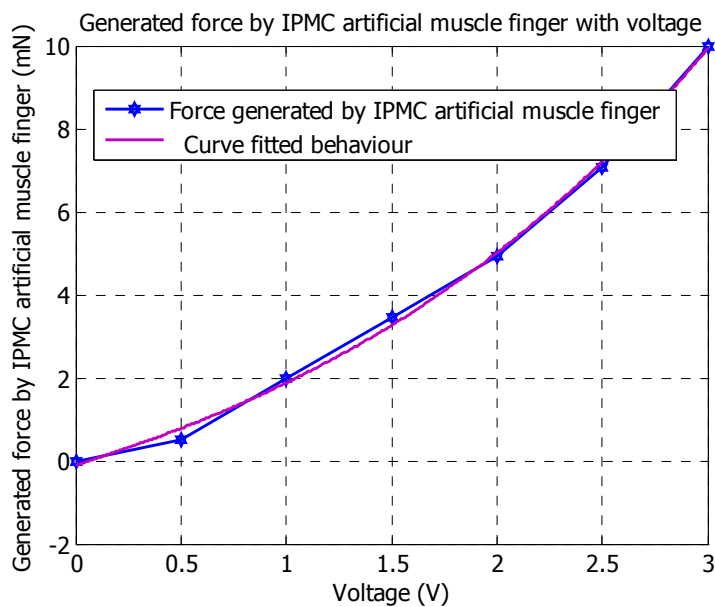


Figure 16. Generated force by IPMC based artificial muscle finger at tip with voltage

The maximum generated force of 10 mN is achieved by IPMC based artificial muscle finger at 45° angle of index finger with cubic polynomial behaviour as shown in Fig. 17. This happens due to human finger behaviour where EIP and EDC muscles are connected with DIP and PIP joints. The generated force (F) by IPMC based artificial muscle finger at tip in term of human finger angle (θ) is also obtained as under

$$F(\theta) = -0.000083 \times \theta^3 + 0.01 \times \theta^2 - 0.063 \times \theta + 0.045 \quad (\text{in mN}) \quad (11)$$

For observing the real time IPMC based artificial muscle finger behaviour with moving human finger angle, experiments are conducted and data are plotted as shown in Fig. 18 and it shows almost proportional behaviour with quadratic relationship. This occurs due to human finger behaviour where EIP and EDC are connected with IO and LU muscles (Fig. 3).

The relationship between IPMC based artificial muscle finger displacement (δ) and human finger angle (θ) is given below,

$$\delta(\theta) = -0.0016 \times \theta^2 + 0.34 \times \theta - 0.15 \quad (\text{in mm}) \quad (12)$$

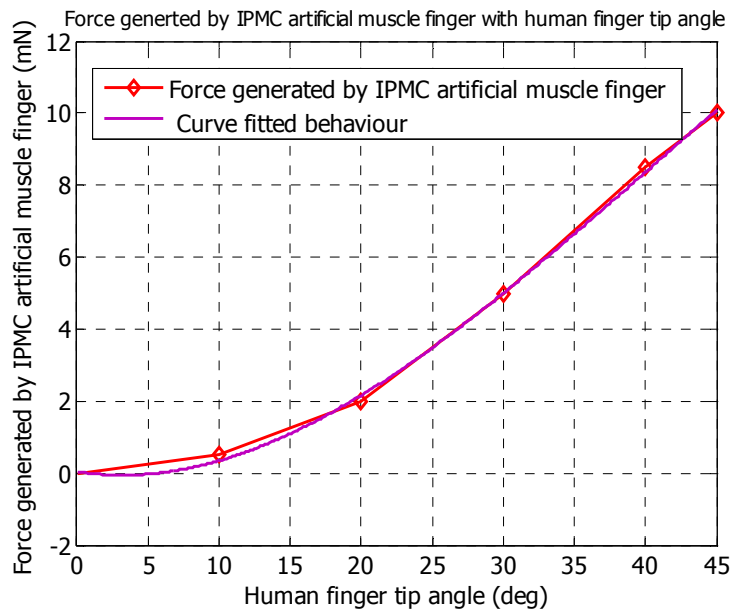


Figure 17. Generated force by IPMC based artificial muscle finger with human finger angle

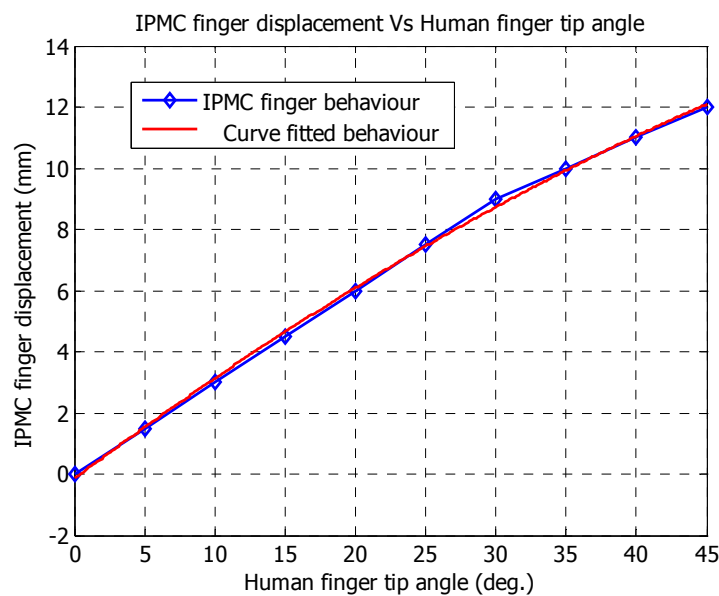


Figure 18. Relationship between IPMC based artificial muscle finger and human finger angle

For actuation of IPMC based artificial muscle finger, the analysis of activated muscles is carried out as given in Table 1. We have analysed different conditions during contraction of different muscles of index finger like intrinsic and extrinsic which are responsible for actuation of IPMC based artificial muscle finger so that they can be used to hold an object.

Cases	Intrinsic muscles			Extrinsic muscles				State	Polarity	
	IO 1	IO 2	LU	EDC	EIP	FDS	FDP		Side A	Side B
1	OFF	OFF	OFF	OFF	OFF	OFF	OFF	None	None	None
2	ON	OFF	ON	OFF	OFF	ON	ON	Adduction	+ive	-ive
3	OFF	ON	ON	ON	ON	OFF	OFF	Abduction	-ive	+ive
4	ON	ON	ON	ON	ON	ON	ON	None	None	None

Table 1. Analysis of different condition of muscles

The two surfaces of IPMC are denoted as side A and side B. In case of intrinsic muscles, the adduction is possible. When IO 1 or IO 2 are in either “on” or “off” condition along with LU muscle in “on” condition then it shows the abduction state. In case of extrinsic muscles, EDC and EIP muscles both are in “off” condition to achieve the adduction state when FDS and FDP muscles both are in “on” condition and for attaining the abduction state EDC and EIP both are in “on” condition when FDS and FDP both are in “off” condition. In rest cases, no power is achieved. Therefore, IPMC based artificial muscle finger is activated in above mentioned conditions from muscles.

The voltage characteristic behavior is taken from EMG and fed to IPMC based artificial muscle finger for actuation in real time environment as shown in Fig. 19. It is found that the trend of IPMC actuation voltage is similar to EMG voltage with amplification factor.

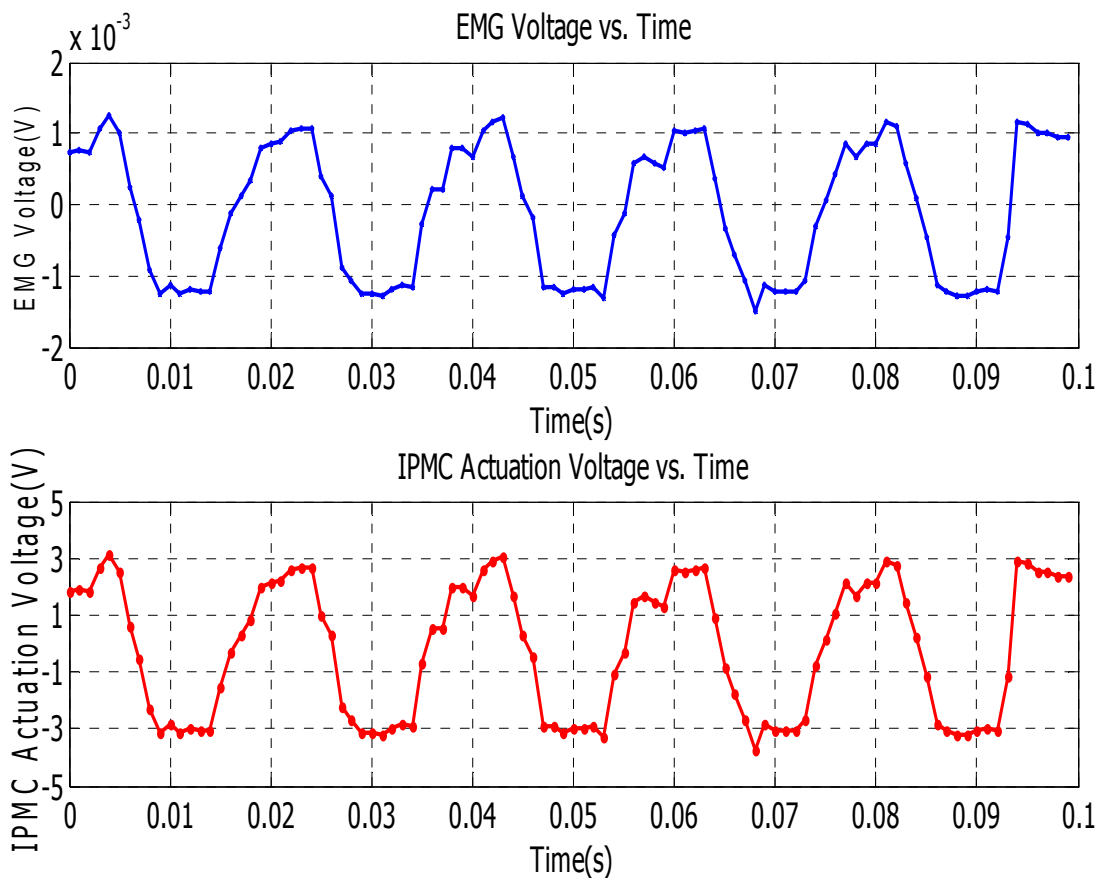


Figure 19. Different voltage responses in real time environment

The EMG voltage $V_{EMG}(t)$ and IPMC actuation voltage $V_{IPMC\ actuation}(t)$ equations are respectively given below,

$$V_{EMG}(t) = \sum V_{0E} \sin(2\pi f_{0E}t + \delta_{0E}), \quad 0 \leq t \leq 0.1 \quad (13)$$

and

$$V_{IPMC\ actuation}(t) = \sum V_{0I} \sin(2\pi f_{0I}t + \delta_{0I}), \quad 0 \leq t \leq 0.1 \quad (14)$$

Where, V_{0E} is average value of EMG voltage (V); f_{0E} is EMG frequency range (Hz); t is signal sample time (s); δ_{0E} is phase difference when signal is taken through EMG (rad); V_{0I} is average value of IPMC actuation voltage (V); f_{0I} is IPMC actuation frequency range (Hz); δ_{0I} is phase difference when signal is given to IPMC (rad). For finding the frequency range of each signal, the experimental data are taken and solved through MATLAB curve fitting tool. The numerical values are $V_{0E} = 0.001451 \pm 0.0002707$ V, $f_{0E} = 4.7 \pm 0.006201$ Hz, $\delta_{0E} = -1.736 \pm 0.036$ rad, $V_{0I} = 2.493 \pm 0.208$, $f_{0I} = 48.5 \pm 0.65$ and $\delta_{0I} = -10.5732 \pm 0.6556$ rad. From these data, it is found that EMG frequency range (f_{0I}) is similar to simulated data and IPMC actuation frequency range is 48.5 ± 0.65 Hz which is in between human muscle frequency range (48-52Hz).

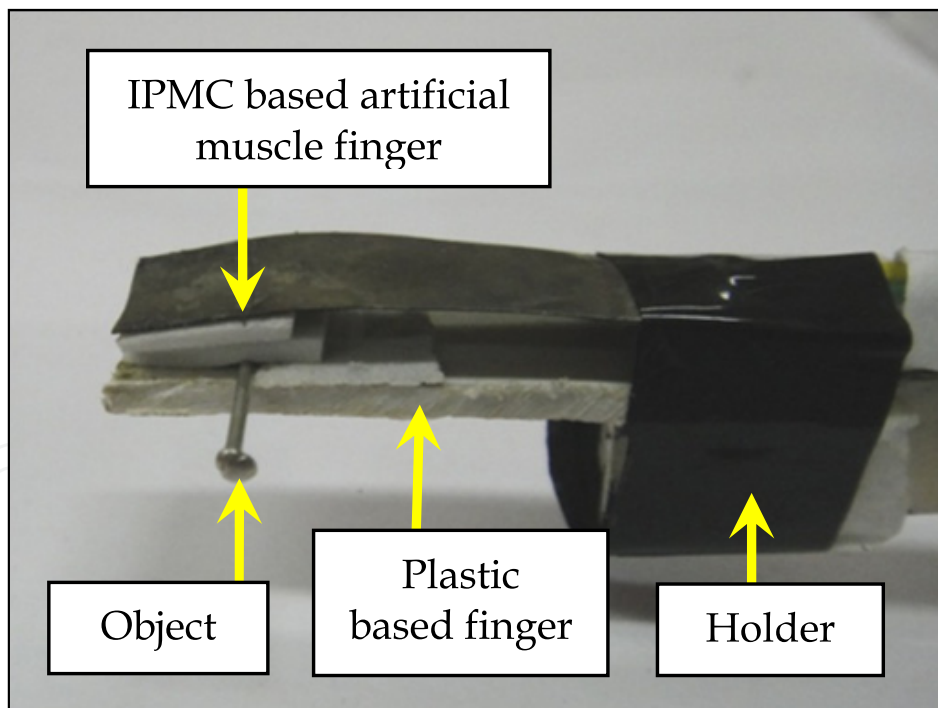


Figure 20. IPMC based artificial muscle finger based micro gripper driven by EMG

After these analyses, an IPMC artificial muscle finger based micro gripper is developed which is driven by EMG as shown in Fig. 20 where one IPMC based artificial muscle finger and other plastic based finger are fixed with double sided tape within one holder. The IPMC based artificial muscle finger is connected through copper tape and wire with EMG sensor

so that an IPMC based artificial muscle finger is activated by EMG signal via human finger. The packing tape is also placed on the tip of IPMC based artificial muscle finger so that this finger perfectly holds the object like micro pin for assembly. After these observations, it is understood that IPMC finger behaves as an artificial muscle and this characteristic is implemented in the development of IPMC artificial muscle finger based micro gripper for holding the object through EMG. The major advantages of EMG-driven IPMC based artificial muscle finger are low voltage in man-machine interface, large bending amplitude and simple control that are applied in development of micro/bio robot.

6. Conclusion

In order to develop the micro/bio-mimetic robot for micro assembly, the potential of an EMG driven artificial finger is discussed in this chapter. An artificial finger for micro assembly is designed using IPMC where IPMC is used as an active artificial finger for holding the object. An IPMC has several advantages such as actuating through a small voltage (± 3 V), light in weight, flexible in nature and does not involve sophisticated controllers for operation. For activating the IPMC based artificial finger, voltage is taken from human index finger through EMG sensor instead of battery source as this is used as a man-machine interface device. Principally, EMG sensor acquires the signal from body during expansion or contraction of muscles. These movements are transferred into an IPMC based artificial muscle finger. For achieving the stable data from EMG, different configurations of control methods are analysed. A PID control system is implemented for attaining the noiseless and stable signal from the user's myoelectric signal. While acquiring the data, a differential amplification technique is applied where data is filtered through a band pass filter and noise is eliminated through three band stop filters. For sending this signal to the IPMC, an algorithm has been developed in Labview software which gives emphasis on following points:

- Acquire voltage data (± 1.2 mV) from human index finger using EMG sensor through data acquisition system
- Amplify the continuous EMG signal through DAQ assistant enabling the filter and domain frequency range options
- Activate IPMC finger through amplified data (± 3 V) using interface device for functioning as artificial muscle finger

Experimentally, it is demonstrated that IPMC based artificial muscle finger is capable of adopting this voltage from EMG signal and mimics as a human finger. From application point of view, an IPMC artificial finger based micro gripper is developed and its capability is also verified. Through this demonstration, it is proved that IPMC can be activated through EMG signal and is applicable as flexible and compliant finger for holding the object in the fields of micro manipulation. IPMC based artificial muscle could also be a replacement of an electro-mechanical system like electric motors in the application field of rehabilitation technology.

7. Future direction

In future, we will focus on developing well equipped EMG driven micro robotic system where IPMC based micro robotic arm along with multiple IPMC artificial fingers will be used. IPMC based micro robotic arm will be operated through human fore arm movement for lifting and manipulation. Multiple IPMC fingers will be used for robust application like grasping, holding and mimicking of a human hand. Therefore, this new generation of robotic system can be really operated in real world through humans using EMG signals.

Author details

R.K. Jain*, S. Datta and S. Majumder

*Design of Mechanical System Group/Micro Robotics Laboratory,
CSIR-Central Mechanical Engineering Research Institute (CMERI),
Durgapur, West Bengal, India*

Acknowledgement

The authors are grateful to the Director, Central Mechanical Engineering Research Institute (CMERI), Durgapur, West Bengal, India for providing the permission to publish this book chapter. This work is financially supported by the Council of Scientific and Industrial Research (CSIR), New Delhi, India under eleventh five year plan on “Modular Re-configurable Micro Manufacturing System (NWP-30)”.

8. References

- Ahmad I., Ansari F. & Dey U. K. (2012). A review of EMG recording technique, *International Journal of Engineering Science and Technology*, Vol. 4, No. 2, pp. 530-539.
- Andreasen D. S., Allen S. K. & Backus D. A. (2005). Exoskeleton with EMG based active assistance for rehabilitation, *Proceedings of the 2005 IEEE 9th International Conference on Rehabilitation Robotics*, Chicago, IL, USA, June 28 - July 1, pp. 333-336.
- Andrews J. (2008). Finger movement classification using forearm EMG signals, *MS Thesis*, Queen's University, Kingston Ontario, Canada.
- Aravinthan P., GopalaKrishnan N., Srinivas P. A. & Vigneswaran N. (2010). Design, development and implementation of neurologically controlled prosthetic limb capable of performing rotational movement, *IEEE International Conference RFID 2010*, Orlando, USA, 14-16April, pp. 241-244.
- Arieta H., Katoh R., Yokoi H. & Wenwei Y. (2006). Development of a multi-DOF electromyography prosthetic system using the adaptive joint mechanism, *ABBI 2006*, Vol. 3, No. 2, pp. 1-10.

* Corresponding Author

- Artemiadis P. K. & Kyriakopoulos K. J. (2010). EMG-based control of a robot arm using low-dimensional embeddings, *IEEE Transactions on Robotics*, Vol. 26, No. 2, pp. 393-398.
- Artemiadis P. K. & Kyriakopoulos K. J. (2011). A switching regime model for the EMG-based control of a robot arm, *IEEE Transactions on Systems, Man and Cybernetics—Part B: Cybernetics*, Vol. 41, No. 1, pp. 53-63.
- Banks J. L. (2001). Design and control of an anthropomorphic robotic finger with multi-point tactile sensation, *MS Thesis*, Artificial Intelligence Laboratory Massachusetts Institute of Technology.
- Bar-Cohen Y. (2002). Electro-active polymers: current capabilities and challenges, *Proceedings of the SPIE Smart Structures and Materials Symposium EAPAD Conference* San Diego CA, 18-21 March, paper no 4695-02.
- Biddiss E. & Chau T. (2006). Electroactive polymeric sensors in hand prostheses: bending response of an ionic polymer metal composite, *J. of Medical Engineering & Physics*, Vol. 28, pp. 568-578.
- Bitzer S. & Smagt P. V. (2006). Learning EMG control of a robotic hand: towards active prostheses, *Proceedings of the 2006 IEEE International Conference on Robotics and Automation*, Orlando, Florida.
- Blouin J., Guillaud E., Bresciani J. P., Guerraz M. & Simoneau M. (2010). Insights into the control of arm movement during body motion as revealed by EMG analyses, *J. of Brain Research*, Vol. 1309, pp. 40-52. Available: <http://www.sciencedirect.com>
- Bundhoo V. & Park E. J. (2005). Design of an artificial muscle actuated finger towards biomimetic prosthetic hands, *IEEE 12th International Conference on Advanced Robotics (ICAR)* Seattle WA, 18-20 July, pp. 368-370.
- Bundhoo V., Haslam E., Birch B. & Park E. J. (2008). A shape memory alloy-based tendon-driven actuation system for biomimetic artificial fingers part I: design and evaluation, *J. of Robotica*, pp. 1-16.
- Cesqui B., Krebs H. I. & Micera S. (2008). On the development of a new EMG-controlled robot-mediated protocol for post-stroke neurorehabilitation, *Proceeding ISG 08*. <http://www.gerontechnology.info/Journal/Proceedings/ISG08/papers/130.pdf>
- Chan A., Kwok E. & Bhuanantanondh P. (2012). Performance assessment of upper limb myoelectric prostheses using a programmable assessment platform, *J. Med. Biol. Eng.*, (In press)
- Chen C. C., Hsueh Y. H. & He Z. C. (2008). A Novel EMG Feedback Control Method in Functional Electrical Stimulation Cycling System for Stroke Patients, *World Academy of Science, Engineering and Technology*, Vol. 42, pp. 186-189.
- Chen Z., Um T. I. & Smith H. B. (2011). A novel fabrication of ionic polymer-metal composite membrane actuator capable of 3-dimensional kinematic motions, *Sensors and Actuators*, Vol. A 168, pp. 131-139.
- Cheron G., Draye J. P., Bourgeois M. & Libert G. (1996). A dynamic neural network identification of electromyography and arm trajectory relationship during complex movements, *IEEE Transactions on Biomedical Engineering*, Vol. 43, No. 5, pp. 552-558.

- Cocaud C. & Jnifene A. (2003). Analysis of a two DOF anthropomorphic arm driven by artificial muscles, *Proceedings of the IEEE International Workshop on Haptic, Audio and Visual Environments and Their Applications (HAVE 2003)*, Ottawa, Ontario, Canada, September 21-22, pp. 37-42.
- Crawford B., Miller K., Shenoy P. & Rao R. P. N. (2005). Real-time classification of electromyographic signals for robotic control, *Proceedings of AAAI*, pp. 523-528.
- Dalley S. A., Wiste T. E., Withrow T. J. & Goldfarb M. (2009). Design of a multifunctional anthropomorphic prosthetic hand with extrinsic actuation, *IEEE/ASME Transactions on Mechatronics*, pp. 1-8.
- DeLaurentis K. J. & Mavroidis C. (2002). Mechanical design of a shape memory alloy actuated prosthetic hand, *Technology and Health Care*, Vol. 10, pp. 91-106.
- DoNascimento B. G., Vimieiro C. B. S., Nagem D. A. P. & Pinotti M. (2008). Hip orthosis powered by pneumatic artificial muscle voluntary activation in absence of myoelectrical signal, *Artificial Organs*, Vol. 32, No. 4, pp. 317-322, Blackwell Publishing, Inc. © 2008.
- Frigo C., Ferrarin M., Frasson W., Pavan E. & Thorsen R. (2007). EMG signals detection and processing for on-line control of functional electrical stimulation, *J. of Electromyography and Kinesiology*, Vol. 10, pp. 351-360.
- Fukuda O., Tsuji T., Kaneko M. & Otsuka A. (2003). A human-assisting manipulator teleoperated by EMG signals and arm motions, *IEEE Transactions on Robotics and Automation*, Vol. 19, No. 2, pp. 210-222.
- Gandole Y. B. (2012). Noise reduction of biomedical signal using artificial neural network model, *International Journal of Engineering and Technology*, Vol. 2, No. 1.
- Gao Z., Lei J., Song Q., Yu Y. & Ge Y. J. (2006). Research on the surface EMG signal for human body motion recognizing based on arm wrestling robot, *Proceedings of the 2006 IEEE International Conference on Information Acquisition*, Weihai Shandong China, 20-23 August, pp. 1269-1273.
- Hao L., Wei F., Lin Y., Zheng P. & Tao W. (2008). Study on a new dexterous hand actuated by pneumatic muscle actuators, *Proceedings of the 7th JFPS International Symposium on Fluid Power*, Toyama, 15-18 September, pp. 521-526.
- Herrera A., Bernal A., Isaza D. & Adjouadi M. (2004). Design of an electrical prosthetic gripper using EMG and linear motion approach, *Florida Conference on Recent Advances in Robotics*, University of Central Florida.
- Hidalgo M., Tene G. & Sánchez A. (2005). Fuzzy control of a robotic arm using EMG signals, *International Conference on Industrial Electronics and Control Applications*, pp. 1-6.
- Hu X. L., Tong K. Y., Song R., Zheng X. J. & Leung W. F. W. (2009). A comparison between electromyography-driven robot and passive motion device on wrist rehabilitation for chronic stroke, *Neuro rehabilitation and Neural Repair*, Vol. 23, No. 8, pp. 837-846, <http://nnr.sagepub.com>.
- Huang H., Zhang F., Sun Y. L. & H. Haibo (2010). Design of a robust EMG sensing interface for pattern classification, *J. Neural Eng.*, Vol. 7, 056005 (10pp).

- Hudgins B., Englehart K., Parker P. & Scott R. N. (1997). A microprocessor-based multifunction myoelectric control system, *CMBE*, Institute of Biomedical Engineering University of New Brunswick Fredericton NB Canada. Available: <http://www.ee.unb.ca/kengleha/papers/CMBES97>.
- Itoh Y., Uematsu H., Nogata F., Nemoto T., Inamori A., Koide K. & Matsuura H. (2007). Finger curvature movement recognition interface technique using SEMG signals, *J. of Achievements in Materials and Manufacturing Engineering (JAMME)*, Vol. 23, No. 2, pp. 43-46.
- Jain R. K., Datta S., Majumder S., A Paul & Banerjee P. (2012). Bio-mimetic behavior of IPMC using EMG signal for micro robot, *International Conference on Micro Actuators and Micro Mechanisms MAMM-2012*, CSIR-CMERI India, January 19-20.
- Jain R. K., Datta S., Majumder S., Chowdhury S. & Banerjee P. (2011). IPMC artificial muscle finger activated through EMG. *Worldwide EAP newsletter on <http://www.EAPnewsletter>*. Vol. 13, No 01, June (The 25th issue), pp.10-12.
- Jain R. K., Datta S., Majumder S., Mukherjee S., Sadhu D., Samanta S. & Benerjee K. (2010b). Bio-mimetic behaviour of IPMC artificial muscles using EMG signal, *ACEEE International Conference in Recent Technologies in Communication and Computing*, Kottayam India, 16-17 October, pp. 186-189.
- Jain R. K., Dutta S. & Majumdar S. (2010a). Control of IPMC-based artificial muscle using EMG signal for hand prosthesis, *Worldwide EAP newsletter on <http://www.EAPnewsletter>*, Vol. 12, No 01, June (The 23th issue), pp.11-13.
- Joshi S. S., Wexler A. S., Maldonado C. P. & Vernon S. (2011). Brain-muscle-computer interface using a single surface electromyographic signal: initial results, *Proceedings of the 5th International IEEE EMBS Conference on Neural Engineering*, Cancun, Mexico, 27April – 1 May, pp. 342-347.
- Khokhar Z. O., Xiao Z. G. & Menon C. (2010). Surface EMG pattern recognition for real-time control of a wrist exoskeleton, *J. of Bio. Med. Eng.*, Vol. 9, No. 41, pp. 1-17.
- Kim K. J. & Shahinpoor M. (2002). A novel method of manufacturing three dimensional ionic polymer metal composites (IPMCs) bio mimetic sensors actuators and artificial muscles, *Polymer*, Vol. 43, pp. 797-802.
- Kottke E. A., Partridge L. D. & Shahinpoor M. (2007). Bio-potential activation of artificial muscles, *J. of Intelligent Material Systems and Structures*, Vol. 18, No. 2, pp. 103-109.
- Kryzstoforski K., Wolczowski A., Bedzinski R. & Helt K. (2004). Recognition of palm finger movements on the basis of EMG signals with the application of wavelets, *Task Quarterly*, Vol. 8, No. 2, pp. 269-280.
- Lau B. G. (2009). An intelligent prosthetic hand using hybrid actuation and myoelectric control, *Ph D Thesis*, The School of Mechanical Engineering, University of Leeds.
- Lee M. J., Jung S. H., Kim G. S., Moon I., Lee S. & Mun M. S. (2007). Actuation of the artificial muscle based on ionic polymer metal composite by electromyography (EMG) signals, *J. of Intelligent Material Systems and Structures*, Vol. 18, pp. 165-170. doi: 10.1177/1045389X06063463.

- Lee M. J., Jung S. H., Lee S., Mun M. S. & Moon I. (2006). Control of IPMC-based artificial muscle for myoelectric hand prosthesis, *The First IEEE/RAS-EMBS International Conference on Biomedical Robotics and Biomechatronics BioRob 2006*, 20-22 February, pp. 1172-1177.
- Lee S., Noh S., Lee Y. & Park J. H. (2009). Development of bio-mimetic robot hand using parallel mechanisms, *Proceedings of the 2009 IEEE International Conference on Robotics and Biomimetics*, Guilin China, 19 -23 December, pp. 550-555.
- Li L., Looney D., Park C., Rehman N. U., & Mandic D. P. (2011). Power independent EMG based gesture recognition for robotics, *IEEE Engineering in Medicine and Biology Magazine*, pp. 793-796.
- Light C. M., Chappell P. H., Hudgins B. & Englehart K. (2002). Intelligent multifunction myoelectric control of hand prostheses, *J. of Medical Engineering & Technology*, Vol. 26, No. 4, July/August, pp. 139-146.
- Luo R. C. & Chang C. C. (2010). Electromyographic signal integrated robot hand control for massage therapy applications, *IEEE/RSJ International Conference on Intelligent Robots and Systems*, Taipei, Taiwan, October 18-22, pp. 3881-3886.
- Matsubara T., Hyon S. H. & Morimoto J. (2011). Learning and adaptation of a stylistic myoelectric interface: EMG-based robotic control with individual user differences, *IEEE International Conference on Robotics and Biomimetics (ROBIO)*, Phauket Island, Thailand, 7-11 December, pp. 390-395.
- Mobasser F. & Hashtrudi-Zaad K. (2005). Rowing stroke force estimation with EMG signals using artificial neural networks, *IEEE International Conference on Control Application (CCA-2005)*, 28-31 August, pp. 825-830.
- Murphy C., Campbell N., Caulfield B., Ward T. & Deegan C. (2008). Micro electro mechanical systems based sensor for mechanomyography, *19th International Conference on Bio-Signal*, Brno, Czech Republic.
- Naik G. R., Kumar D. K. & Arjunan S. P. (2010). Pattern classification of myo-electrical signal during different maximum voluntary contractions: a study using BSS techniques, *Measurement Science Review*, Vol. 10, No. 1, pp. 1-6.
- O'Toole K. T. & McGrath M. M. (2007). Mechanical design and theoretical analysis of a four fingered prosthetic hand incorporating embedded SMA bundle actuators, *World Academy of Science Engineering and Technology*, Vol. 31, pp. 142-149.
- Peleg D., Braiman E., Yom-Tov E. & Inbar G. F. (2002). Classification of finger activation for use in a robotic prosthesis arm, *IEEE Transactions on Neural Systems and Rehabilitation Engineering*, Vol. 10, No. 4, pp. 290-293.
- Pfeiffer C., DeLaurentis K. & Mavroidis C. (1999). Shape memory alloy actuated robot prostheses: initial Experiments, *Proceedings of IEEE International Conference on Robotics and Automation*, Vol. 3, pp. 2385-2391.
- Pittaccio S. & Viscuso S. (2011). An EMG-controlled SMA device for the rehabilitation of the ankle joint in post-acute stroke, *Journal of Materials Engineering and Performance*, Vol. 20, No.4-5, pp. 666-670.

- Qi L., Wakeling J., Grange S. & Ferguson-Pell M. (2012). Changes in surface electromyography signals and kinetics associated with progression of fatigue at two speeds during wheelchair propulsion, *JRRD*, Vol. 49, No. 1, pp. 23–34.
- Rosen J., Brand M., Fuchs M. B. & Arcan M. (2001). A myosignal-based powered exoskeleton system, *IEEE Transaction on Systems, Man and Cybernetics—Part A: Systems and Humans*, Vol. 31, No. 3, pp. 210-222.
- Roy S. H., Luca G. D., Cheng M. S., Johansson A., Gilmore L. D. & Luca C. J. D. (2007). Electro-mechanical stability of surface EMG sensors, *J. of Med. Bio. Eng. Comput.*, Vol. 45, pp. 447-457
- Saponas T. S., Tan D. S., Morris D. & Balakrishnan R. (2008). Demonstrating the feasibility of using forearm electromyography for muscle-computer Interfaces, *CHI 2008*, Florence Italy, 5-10 April.
- Shahinpoor M. & Kim K. J. (2001). Ionic polymer–metal composites: I. Fundamental, *Smart Materials Structure*, Vol. 10, pp. 819–833.
- Shahinpoor M. & Kim K. J. (2004). Ionic polymer–metal composites: III. Modeling and simulation as biomimetic sensors actuator transducer and artificial muscles, *Smart Materials Structure*, Vol. 13, pp. 1362-1388.
- Shenoy P., Miller K. J., Crawford B. & Rao R. P. N. (2008). Online electromyographic control of a robotic prosthesis, *IEEE Transactions on Biomedical Engineering*, Vol. 55, No. 3, pp. 1128-1135.
- Stirling L., Yu C. H., Miller J., Hawkes E., Wood R., Goldfield E. & Nagpal R. (2011). Applicability of shape memory alloy wire for an active soft orthotic, *Journal of Materials Engineering and Performance*, Vol. 20, Issue 4-5, pp. 658-662.
- Sun Y. P., Yen K. T., Kung H. K., Tsai Y. C., Lu K. C., Du C. M. & Liang Y. C. (2012). The muscular function for human knee movement revealed from electromyography: a preliminary study, *Life Science Journal*, Vol. 9, No. 1, pp. 453-456.
- Thayer N. & Priya S. (2011). Design and implementation of a dexterous anthropomorphic robotic typing (DART) hand, *Smart Mater. Struct.*, Vol. 20, pp. 035010 (12pp).
- Vogel J., Castellini C., & Smagt P. V. (2011). EMG-based teleoperation and manipulation with the DLR LWR-III, *IEEE/RSJ International Conference on Intelligent Robots and Systems*, San Francisco, CA, USA, September 25-30, pp. 672-678.
- Wege A. & Zimmermann A. (2007). Electromyography (EMG) sensor based control for a hand exoskeleton, *Proceedings of the 2007 IEEE International Conference on Robotics and Bio-mimetics*, Sanya China, 15 -18 December, pp. 1470-1475.
- Wheeler K. R. (2003). Device control using gestures sensed from EMG, *IEEE International Workshop on Soft Computing in Industrial Applications*, Binghamton University, Binghamton, New York, June 23-25, 2003.
- Yagiz N., Arslan Y. Z. & Hacıoglu Y. (2007). Sliding mode control of a finger for a prosthetic hand, *J. of Vibration and Control*, Vol. 13, No. 6, pp. 733–749, doi: 10.1177/1077546307072352.

Zollo L., Roccella S., Guglielmelli E., Carrozza M. C. & Dario P. (2007). Biomechatronic design and control of an anthropomorphic artificial hand for prosthetic and robotic applications, *IEEE/ASME Transactions on Mechatronics*, Vol. 12, No. 4, pp. 418-429.

IntechOpen

IntechOpen